

Research Article

Numerical Simulation of Temperature and Flow Field in Horizontal Continuous Annealing Furnace

Su Fu-Yong and Li Zhi

School of Mechanical Engineering, University of Science and Technology Beijing (USTB), Beijing, 100083, China

Abstract: This study aims to get the temperature field and flow field of the heating section in a horizontal continuous annealing furnace of hot-rolled stainless strip by using CFD to build a 3-D simulation model. The simulation results are compared with measured data and the accuracy of the model is proved by the predicted temperature distribution. On this basis, focus on the distribution and variation of convective heat transfer coefficient and equivalent radiation heat transfer coefficient of the strip surface. All the researches have great significance on further developing the mathematical model of horizontal continuous annealing furnace of stainless strip and optimizing the controlling strategy.

Keywords: CFD, continuous annealing furnace, numerical simulation, stainless strip

INTRODUCTION

The continuous annealing process of strip steel is used to improve the required physical and mechanical properties of strip steel. The research of annealing and pickling line for stainless steel is mainly about the device configuration and hardware controlling, it is lack for in-depth study about heat transfer mechanism during annealing (Wang and Bai, 2006; Bian *et al.*, 2004). According to the production process, the furnace studied can be divided into four main sections: preheating section, heating section, slow cooling section and fast cooling section, all sections are shown in Fig. 1. In this study, we have done researches of temperature field, flow field and concentration field, as while as the surface heat transfer of the strip by using CFD numerical simulation technology.

Object: Heating section length is 74.8 m and it can be divided into four chambers which are connected end to end, the length of each chamber is 18.7 m and the width is 1.6 m and the height is 1.85 m. The stainless strip goes into the heating section from the head of the first chamber and out from the end of the fourth chamber, meanwhile the gas flows in the opposite direction, which goes out from the head of the first chamber. The head and the end of Chamber 1 and the head of Chamber 2 are higher than other area and it's shown in Fig. 2. The heating section uses open flame to heat the strip, there are 126 burners equipped on the side walls of the furnace and each one has 1 fuel inlet, 4 primary air inlets and 3 secondary air inlets. The number and

individual segments of the burners in each chamber are shown in Table 1.

Select No.304 stainless steel with the width is 1.52 m as the product. It is hanged freely in the furnace. As the strip may change in shape and heating condition while being contacted with the steel roller, in each chamber, we have ignored the strip at the head and the end along the chamber length of 0.2 m and just focused on the 18.3 m left.

MATHEMATICAL MODELS

In order to reflect the laws of the furnace heat exchange, we have carried out some simplified assumptions of the basic physical objects (Carvalho *et al.*, 2006).

Basic assumptions:

- The gas is incompressible
- The processes of flowing and combustion are steady
- There is no air suction and air leakage in the furnace, all the burning gas goes out of the furnace head and into the previous chamber.

Control equations:

- Continuity equation and momentum equation:

$$\frac{\partial \rho}{\partial t} + \nabla \cdot (\rho \bar{u}) = 0 \quad (1)$$

Corresponding Author: Su Fu-Yong, School of Mechanical Engineering, University of Science and Technology Beijing (USTB), Beijing, 100083, China

This work is licensed under a Creative Commons Attribution 4.0 International License (URL: <http://creativecommons.org/licenses/by/4.0/>).

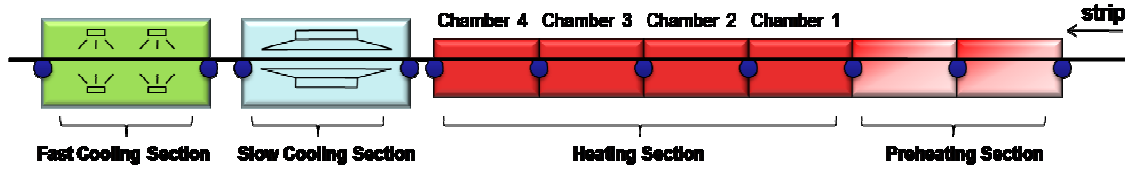


Fig. 1: The production process of continuous annealing

Table 1: Distribution of the burners in different heating chambers

Chamber number	Burner (470 kW)	Burner (330 kW)	Heat input (MW)
1	36	0	16.92
2	36	0	16.92
3	18	18	14.40
4	18	0	8.64
Total	108	18	56.88

Table 2: Gas and air flow of each chamber

Chamber number	Gas flow (m ³ /h)	Air flow (m ³ /h)
1	1039.01	10920.93
2	1187.14	12615.07
3	1019.85	10658.14
4	308.80	3688.57

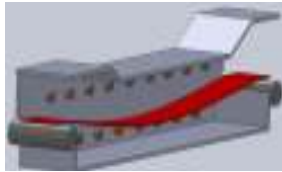


Fig. 2: 3-D model of Chamber 1 of the heating section

$$\frac{\partial(\rho\bar{u})}{\partial t} + \nabla \cdot (\rho\bar{u}\bar{u}) = -\nabla \cdot P + \nabla \cdot (\mu \cdot \text{grad}\bar{u}) + \bar{F} \quad (2)$$

- Energy equation:

$$\frac{\partial(\rho T)}{\partial t} + \nabla \cdot (\rho\bar{u}T) = \nabla \cdot \left(\frac{k}{c_p} \cdot \text{grad}T \right) + S_T \quad (3)$$

- Turbulence model:

Use k-ε model (Bray *et al.*, 1984; Guo *et al.*, 2010), in which turbulent kinetic energy equation is:

$$\frac{\partial(\rho k)}{\partial t} + \nabla \cdot (\rho\bar{u}k) = \nabla \cdot \left[\left(\mu + \frac{\mu_t}{\sigma_k} \right) \nabla \cdot k \right] + G_k + G_b - \rho\varepsilon \quad (4)$$

Turbulent kinetic energy dissipation rate equation is:

$$\frac{\partial(\rho\varepsilon)}{\partial t} + \nabla \cdot (\rho\bar{u}\varepsilon) = \nabla \cdot \left[\left(\mu + \frac{\mu_t}{\sigma_\varepsilon} \right) \nabla \cdot \varepsilon \right] + C_1 \frac{\varepsilon}{k} (G_k - C_3 G_b) - C_2 \rho \frac{\varepsilon^2}{k} \quad (5)$$

From formula (1) to formula (5):

- \bar{u} = The velocity vector
- P = The stress tensor
- \bar{F} = The other mass force
- S_T = The source term of the chemical reactions and other volumetric heat sources

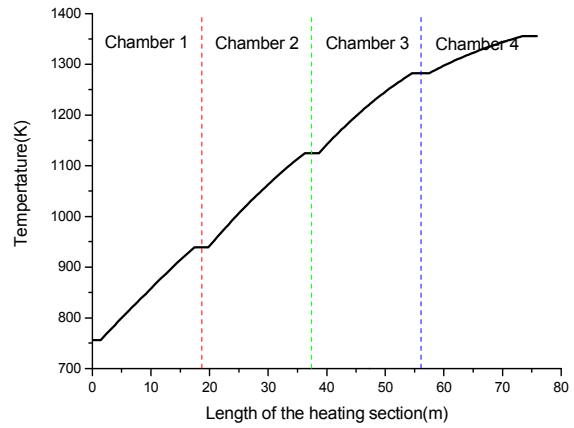


Fig. 3: Temperature of strip along the heating section

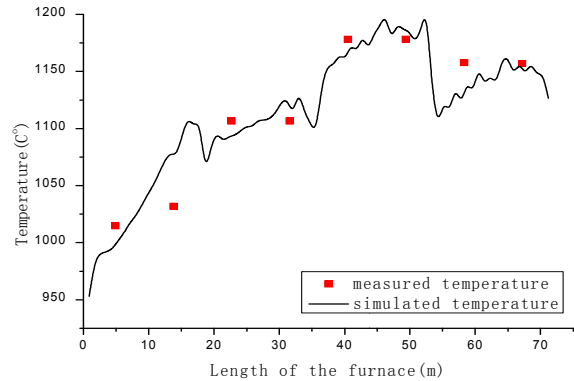


Fig. 4: Comparison of simulated and measured temperature

- μ = Turbulent viscosity
- $\text{Pa}\cdot\text{s}$. G_k = The term produced by shear force
- G_b = The term produced by volume force. $\sigma_T, \sigma_k, C_1, C_2, C_3$ are all constants.

Use Non-premixed combustion model as the combustion model, Discrete Ordinates model as the radiation model.

Boundary conditions: Considering the quantity and the quality of the model grid, we have studied the heating section chamber by chamber and set the boundary conditions chamber by chamber, too. All the boundary conditions settings are similar.

Inlet boundary: This includes gas inlet, flue gas inlet, primary air inlet and secondary air inlet; all these

boundary conditions are set as velocity inlet boundary conditions. Temperature of the air is set as 673 K and the gas is set as 300 K. Table 2 shows gas and air flow of each chamber.

Outlet boundary: Use pressure outlet boundary condition, set the outlet pressure as -200 Pa, reflux temperature as 1473 K.

Boundary conditions of top, bottom and side walls are all set as no-slip boundary conditions, blackness is set as 0.8, radiation heat flux are set as constants.

Both the top and bottom surfaces of the strip boundary conditions are set as no-slip boundary conditions and the blackness is set as 0.35 and the temperature is set according to actual results, which changes with the length of the furnace and is showed in Fig. 3.

NUMERICAL SOLUTION OF MATHEMATICAL MODEL

Results of the furnace temperature field simulation: Figure 4 shows the temperature simulation results of

heating process in stainless steel horizontal continuous annealing furnace and the measured temperature of the heating process. By comparing two kinds of temperature, we can find out that the trend of simulation results are completely correct and it's maximum relative error compared with measured results is less than 4.4%. In summary, the numerical simulation results are reliable.

The simulated flow field and temperature field of the furnace cross-section is shown in Fig. 5.

Results of the heat convection and radiation coefficient variation of the strip: The heat convection coefficient variations of the strip are shown in Fig. 6. From the Figure above, the upper surface heat transfer coefficient value is smaller than that of the lower surface because of a large number of gas flows near the upper surface and the overhanging of the strip and there is a direct impact on heat transfer coefficient of the area which is near the burners. Generally speaking, we can see that the heat transfer coefficient values fluctuate, which is about $4.5 \text{ W}/(\text{m}^2\cdot\text{K})$ and reduces along the length of the furnace.

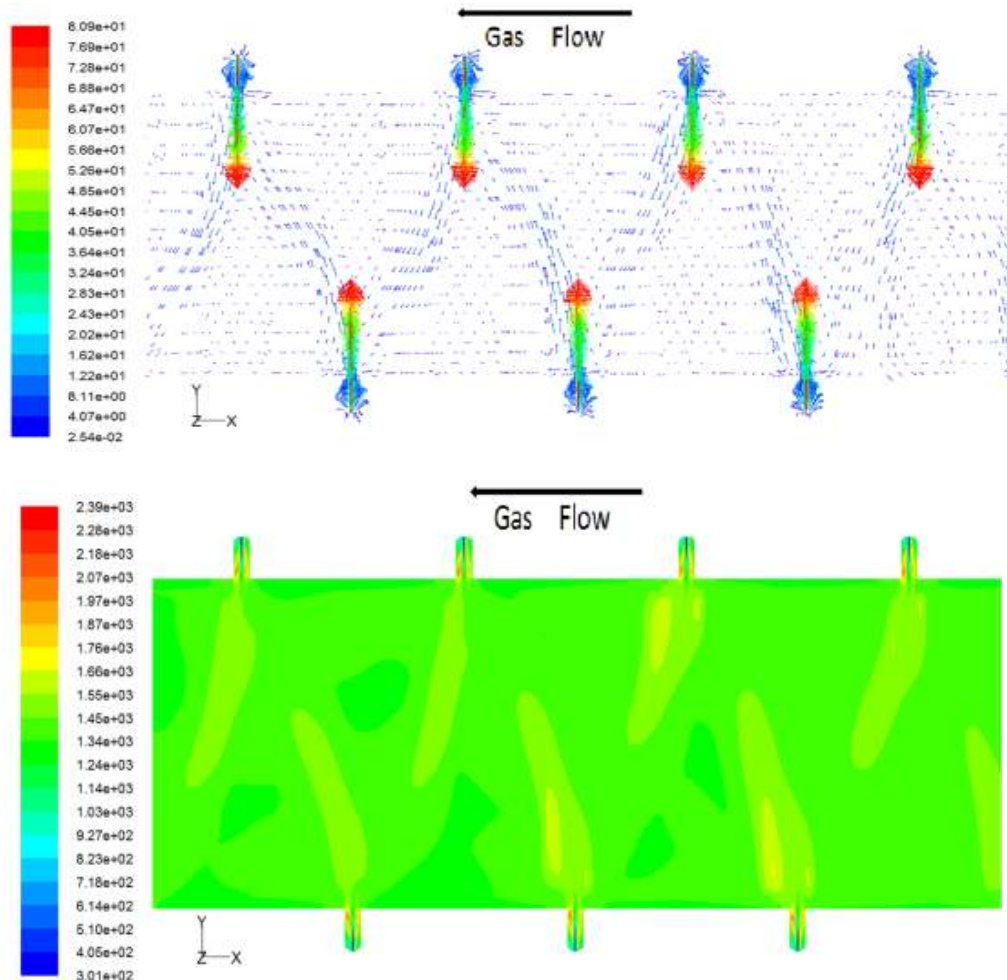


Fig. 5: Flow and temperature field of Chamber 1 cross-section

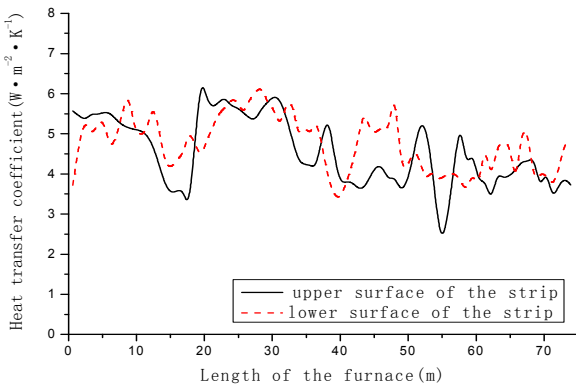


Fig. 6: Convection heat transfer coefficient variation of the strip upper and lower surfaces along length of the furnace

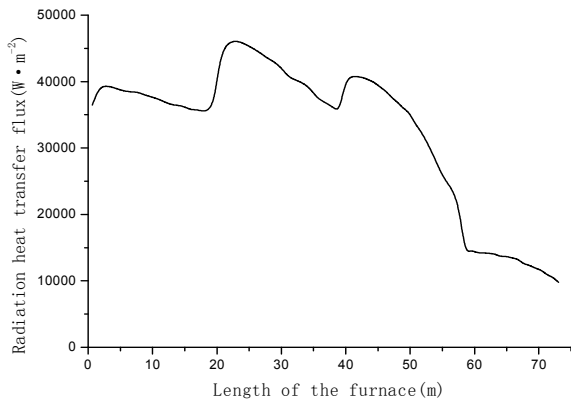


Fig. 7: Radiation heat transfer flux variation of the strip surfaces along length of the furnace

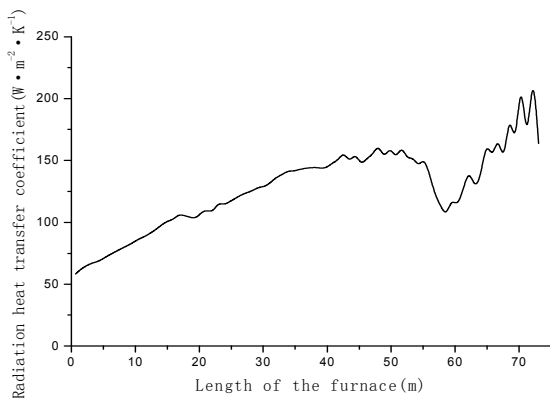


Fig. 8: Equivalent radiation heat transfer coefficient variation of the strip surfaces along length of the furnace

The simulation results can be represented as fitting formulas:

$$\alpha = 4.04(1 + 1.05 \cdot \rho \cdot v) \quad (6)$$

In formula 6, v is the flue gas velocity in the furnace, m/s. and ρ is the flue gas density, kg/m³.

The heat convection coefficient variations of the strip are shown in Fig. 7:

$$h_R = \frac{q_R}{T_g - T_s} \quad (7)$$

In formula 7, q_R is radiation heat transfer flux, W/m². T_g and T_s are the gas temperature and strip temperature at the same position along the strip, K.

Use formula 7 to get the equivalent radiation heat transfer coefficient variation as show in Fig. 8.

Comparing the Fig. 8 and 6, radiation heat transfer coefficient is much larger than the equivalent heat transfer coefficient and the radiation heat transfer flux is also larger than the convective heat transfer flux. We can find out that the radiation heat transfer is the main heat transfer in the furnace.

CONCLUSION

In this study, we have established the physical and mathematical models of heating process in stainless steel horizontal continuous annealing furnace, getting the simulation results of the heating process. After a large number of simulation and verification, the simulation results are similar to the measured values, which prove that the model has achieved very high accuracy. Radiation heat transfer accounts for the major part of heat transfer, while there is a certain amount of convection heat transfer in the furnace. The results achieved have certain significance on the research of the same type of stainless steel annealing furnace.

REFERENCES

- Bian, J., F.B. Zhang, X.H. Liu and G.D. Wang, 2004. Continuous annealing technology for hot-dip galvanization in China. Heat Treat. Metal., 29: 13-16.
- Bray, K.N.C., P.A. Libby and J.B. Moss, 1984. Unified modeling approach for premixed turbulent combustion-Part I: General formulation. Comb. Flame, 61: 87-102.
- Carvalho, S.R., T.H. Ong and G. Guimaraes, 2006. A mathematical and computational model of furnaces for continuous steel strip processing. J. Mater Process. Tech., 178: 379-387.
- Guo, L., C. Yu and X. Liu, 2010. Numerical simulation on gas flow in honeycomb regenerator. Energ. Metall. Ind., 6: 18-21.
- Wang, F.K. and X.Y. Bai, 2006. Overview of annealing furnace for cold rolled stainless steel strip. Ind. Furnace, 28: 18-20.